Chinese Journal of Oceanology and Limnology
Vol. 33 No. 5, P. 1132-1141, 2015
http://dx.doi.org/10.1007/s00343-015-4147-1

A new modulation transfer function for ocean wave spectra retrieval from X-band marine radar imagery*

CHEN Zhongbiao (陈忠彪)[1], ZHANG Biao (张彪)[1, **], HE Yijun (何宜军)[1],
QIU Zhongfeng (丘仲锋)[1], PERRIE William[2]

[1] *Nanjing University of Information Science and Technology, Nanjing 210044, China*
[2] *Bedford Institute of Oceanography, Dartmouth, B2Y4A2, Canada*

Received May 11, 2014; accepted in principle Aug. 25, 2014; accepted for publication Sep. 30, 2014

Abstract When imaging ocean surface waves by X-band marine radar, the radar backscatter from the sea surface is modulated by the long surface gravity waves. The modulation transfer function (MTF) comprises tilt, hydrodynamic, and shadowing modulations. A conventional linear MTF was derived using HH-polarized radar observations under conditions of deep water. In this study, we propose a new quadratic polynomial MTF based on VV-polarized radar measurements taken from heterogeneous nearshore wave fields. This new MTF is obtained using a radar-observed image spectrum and in situ buoy-measured wave frequency spectrum. We validate the MTF by comparing peak and mean wave periods retrieved from X-band marine radar image sequences with those measured by the buoy. It is shown that the retrieval accuracies of peak and mean wave periods of the new MTF are better than the conventional MTF. The results also show that the bias and root mean square errors of the peak and mean wave periods of the new MTF are 0.05 and 0.88 s, and 0.32 and 0.53 s, respectively, while those of the conventional MTF are 0.61 and 0.98 s, and 1.39 and 1.48 s, respectively. Moreover, it is also shown that the retrieval results are insensitive to the coefficients in the proposed MTF.

Keyword: X-band marine radar; modulation transfer function; ocean wave spectra

1 INTRODUCTION

The forecasting of ocean surface waves is important for ocean engineering, offshore structural design, and navigation. Many offshore operations are critically dependent on the prevailing sea state, i.e., parameters such as significant wave height, and wave direction and period. In coastal regions, sea state measurements are also required to support weather prediction, wave climate, and ship routing services. X-band marine radar has the capability of observing the ocean surface with high spatial and temporal resolutions, and it has been used widely to measure ocean surface waves (Young et al., 1985; Nieto-Borge et al., 2004, 2008; Cui et al., 2010; Chen et al., 2014), currents (Senet et al., 2008), and winds (Dankert and Horstmann, 2007).

Ocean waves can be imaged by marine radar because the long surface gravity waves modulate the radar backscatter from the sea surface; thus, the small roughness of the sea surface, which is generated by the local wind field, enhances the backscatter of the ocean surface (Lee et al., 1995; Trizna, 1997). At moderate incidence angles, the modulation is mainly due to the tilt and hydrodynamic modulation (Alpers et al., 1981), whereas at grazing incidence, the modulation also stems from the shadowing of the radar beam due to the ocean waves (Wenzel, 1990). These modulation mechanisms contribute to the imaging of surface waves that have wavelengths

* Supported by the National High Technology Research and Development Program of China (863 Program) (No. 2013AA09A505), the National Natural Science Foundation of China (Nos. 41076119, 41176160, 41476158), the Priority Academic Program Development of Jiangsu Higher Education Institutions (PAPD), the Natural Science Youth Foundation of Jiangsu Province (No. BK2012467), the Natural Science State Key Foundation of Jiangsu Province (No. BK2011008), the National Natural Science Youth Foundation of China (No. 41206171), and the Startup Foundation for Introducing Talent of Nanjing University of Information Science and Technology (No. S8113078001)
** Corresponding author: zhangbiao@nuist.edu.cn

Table 1 Configurations of the X-band marine radar used in the study

Property	Value
Polarization	VV
Frequency	9 410 MHz±30 Hz
Pulse width	70 ns
Pulse repetition frequency	3 000 Hz
Transmitted power	25 Kw
Gain	30.2 dB
Antenna beam width at 3 dB	1.2° horizontal, 20.5° vertical
Antenna type	2.4-m slotted wave guide
Antenna rotation speed	24 r/min

greater than twice that of the radar resolution.

For measurements of ocean surface wave using X-band marine radar image sequences, an empirical modulation transfer function (MTF) is required to scale the radar image and ocean wave spectra. By assuming that the wave field has characteristics of spatial homogeneity and temporal stationarity, and according to linear wave theory, Nieto-Borge et al. (2004) developed a linear MTF that utilizes the HH-polarized radar-observed image spectrum and a collocated offshore in situ buoy-measured wave spectrum. However, the linear wave theory might not be appropriate in complex sea states, such as nearshore regions with shoaling waves, or in the extreme conditions of swell and wind-sea interactions of marine storms. Therefore, the MTF is limited to measurements with VV-polarized radar observations of ocean surface waves in coastal regions.

In this study, we aim to develop a new MTF to retrieve the parameters of ocean surface waves using VV-polarized X-band marine radar image sequences acquired in nearshore areas. This paper is organized as follows: in Section 2, the radar data acquisition system and methodology for the MTF derivation are introduced. In Section 3, the experiment and validation are described. Section 4 considers the effects of different MTFs on wave spectra retrieval and discusses the stability of the presented MTF. Finally, the summary and conclusions are given in Section 5.

2 DATA AND METHODOLOGY

This section describes the X-band marine radar data acquisition system, in addition to the methods used for the development of the new MTF using a radar-observed image spectrum and a buoy-measured wave spectrum.

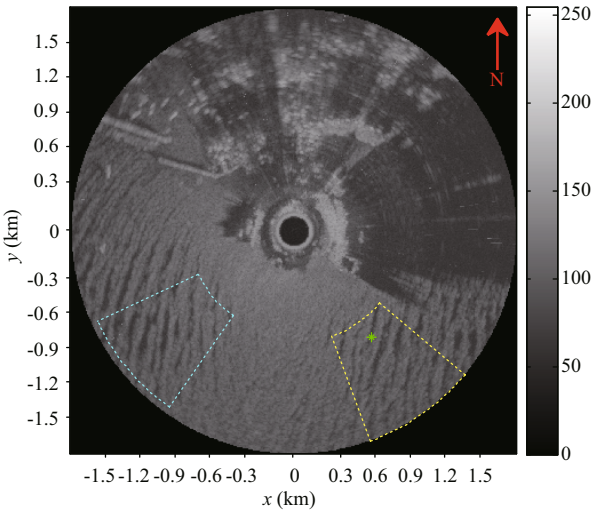

Fig.1 Part of one X-band marine radar image captured at 13:45 UTC on January 3, 2013

The red arrow in the right upper corner denotes north. The northern and southern halves of the image are land and sea, respectively. The green star denotes the buoy location. The yellow and cyan bins are the studied areas Region 1 and Region 2, respectively. The color bar shows the gray levels of the radar image.

2.1 Data acquisition system

The system used to record the radar images is based on the commercial FURUNO X-band nautical radar, the parameters of which are described in Table 1. In order to measure the backscatter from the sea surface, three major changes were applied to the radar: (1) the original antenna's HH polarization was replaced by VV polarization; (2) a dedicated 40-MHz analogue-to-digital converter was implemented on a personal computer to interface the image acquisition system with the radar; (3) software architecture was developed to control the radar and personal computer.

The improved X-band marine radar observed the ocean surface with radial resolution of 3.75 m and azimuthal resolution of approximately 0.05°. The rotation period of the antenna was 2.5 s and 32 images were recorded in each image sequence. As an example, an image captured by the system is shown in Fig.1. The bright and dark stripes in the lower part of the radar image are associated with ocean surface waves traveling east to west. It can be seen that the wave directions and wavelengths change sharply when passing the shore around the radar station, such that the wave field is heterogeneous in the nearshore area. Moreover, no evident ocean wave patterns can be seen on the underface of the radar image, which is because the imaging capacity of the X-band marine radar is reduced when the antenna look angle is perpendicular to the direction of wave propagation.

2.2 Modulation transfer function

To obtain the MTF, the first step is to estimate the 1D wavenumber spectrum $F_r(k)$ from the X-band marine radar image sequence. A grayscale radar image sequence can be denoted as $I(x, y, t)$, where x and y are the coordinates of the image, and t is the acquisition time of the image in the radar image sequence. The radar image sequence is transformed into the image spectrum $\Psi_I(k_x, k_y, \omega)$ by applying the 3D Fast Fourier Transform (FFT):

$$\Psi_r(k_x,k_y,\omega)=\int_{-\infty}^{\infty}\int_{-\infty}^{\infty}\int_{-\infty}^{\infty} I(x,y,t)e^{-i(k_x x+k_y y-\omega t)}\mathrm{d}x\mathrm{d}y\mathrm{d}t\,, \quad (1)$$

where $\vec{k}=(k_x,k_y)$ is the wavenumber vector and ω is angular frequency.

The next step is the extraction of linear gravity wave components from the 3D image spectra. For this, the dispersion relationship that relates the wavenumber to the angular frequency $\omega(\vec{k})$ and the ocean surface current $\vec{U}=(U_x,U_y)$ is used:

$$\omega(\vec{k})=\sqrt{\mathrm{g}k\tanh(kd)}+\vec{k}\cdot\vec{U}\,, \quad (2)$$

where g is gravitational acceleration, d is water depth, and $k=|\vec{k}|=\sqrt{k_x^2+k_y^2}$ is the wavenumber. Taking into account the dispersion relation for linear gravity waves (Eq.2), the 2D filtered image spectrum is estimated as follows (Young et al., 1985):

$$\Psi_r(k_x,k_y)=2\int_{\omega>0}\Psi_r(k_x,k_y,\omega)\delta\left(\omega-\omega(\vec{k})\right)\mathrm{d}\omega\,, \quad (3)$$

where $\delta(\cdot)$ is Dirac's delta function. In the discrete space, the width of the filter depends on the frequency and wavenumber resolutions, which are related to the length of the image time series and the size of the analysis area, respectively. Note that in the following, when we refer to the image spectrum, it is $\Psi_r(k_x,k_y)$ that is considered. It is known that the following is true:

$$\Psi_r(k_x,k_y)=\frac{1}{k}\Psi_r(k,\theta)\,. \quad (4)$$

In addition, the 1D wavenumber spectrum $F_r(k)$ can be estimated using radar measurements:

$$F_r(k)=\int_{\pi}^{\pi}\Psi_r(k_x,k_y)k\mathrm{d}\theta\,. \quad (5)$$

Because of radar wave imaging mechanisms, for example, shadowing and/or tilt modulation (Nieto-Borge, 1997; Seemann, 1997), a difference can be observed between the image spectra from the marine radar imagery and the corresponding spectra from the in situ sensors. However, the use of an MTF can minimize this difference (Plant, 1988; Ziemer and Gunther, 1994). The empirical MTF (Nieto-Borge et al., 2004) can be determined by the following:

$$|M(k)|^2=\frac{F_r(k)}{F_b(k)}\,, \quad (6)$$

where $F_b(k)$ is the 1D wave spectrum derived from the frequency spectrum $S(\omega)$ obtained from the heave time series measured by an in situ buoy:

$$F_b(k)=S[\omega(k)]\frac{\mathrm{d}\omega}{\mathrm{d}k}\,. \quad (7)$$

The shape of the MTF was determined using standard marine radar observations and the pitch-roll WaveScan buoy measurements from the Bay of Biscay campaign (Nieto-Borge et al., 2004). It is worth noting that the radar data were acquired at HH-polarization in a deep-water area (h≈600 m). Under deep-water conditions, the assumption of spatial homogeneity and temporal stationarity of the wave field is valid. However, this hypothesis does not hold in shallow-water regions; for example, in nearshore areas, the wave field is heterogeneous because of topographic effects. In this case, the MTF (Nieto-Borge et al., 2004) is unsuitable for the derivation of ocean wave parameters.

Figure 2a, c, e, g shows the 1D wavenumber spectrum obtained via the in situ buoy measurements and X-band marine radar observations taken under four typical sea states. The wavenumber range is set between 0.03 and 0.31 rad/m. The peak wavenumber differences between the radar derivation and buoy measurements widen as the sea state increases. The reason for this is that shadowing and/or tilt modulation seriously affects the radar imaging of ocean surface waves under high sea states.

Figure 2b, d, f, h shows the estimated MTF (blue lines) based on Eq.6. It is evident that the MTF first decreases and then increases as the wavenumber increases. Therefore, we use a quadratic polynomial function to fit the MTF:

$$\log(|M(k)|^{-2})=p_1\log^2(k)+p_2\log(k)+p_3\,, \quad (8)$$

where $\log(\cdot)$ is the natural logarithm, and p_1, p_2, and p_3 are three coefficients that can be determined by the least squares method.

When the wavenumber ranges between 0.03 and 0.14 rad/m, the MTF decreases with the wavenumber, such that the power decay law of Nieto-Borge et al. (2004) can be used to determine the MTF:

$$|M(k)|^{-2}\propto k^{\beta}\,, \quad (9)$$

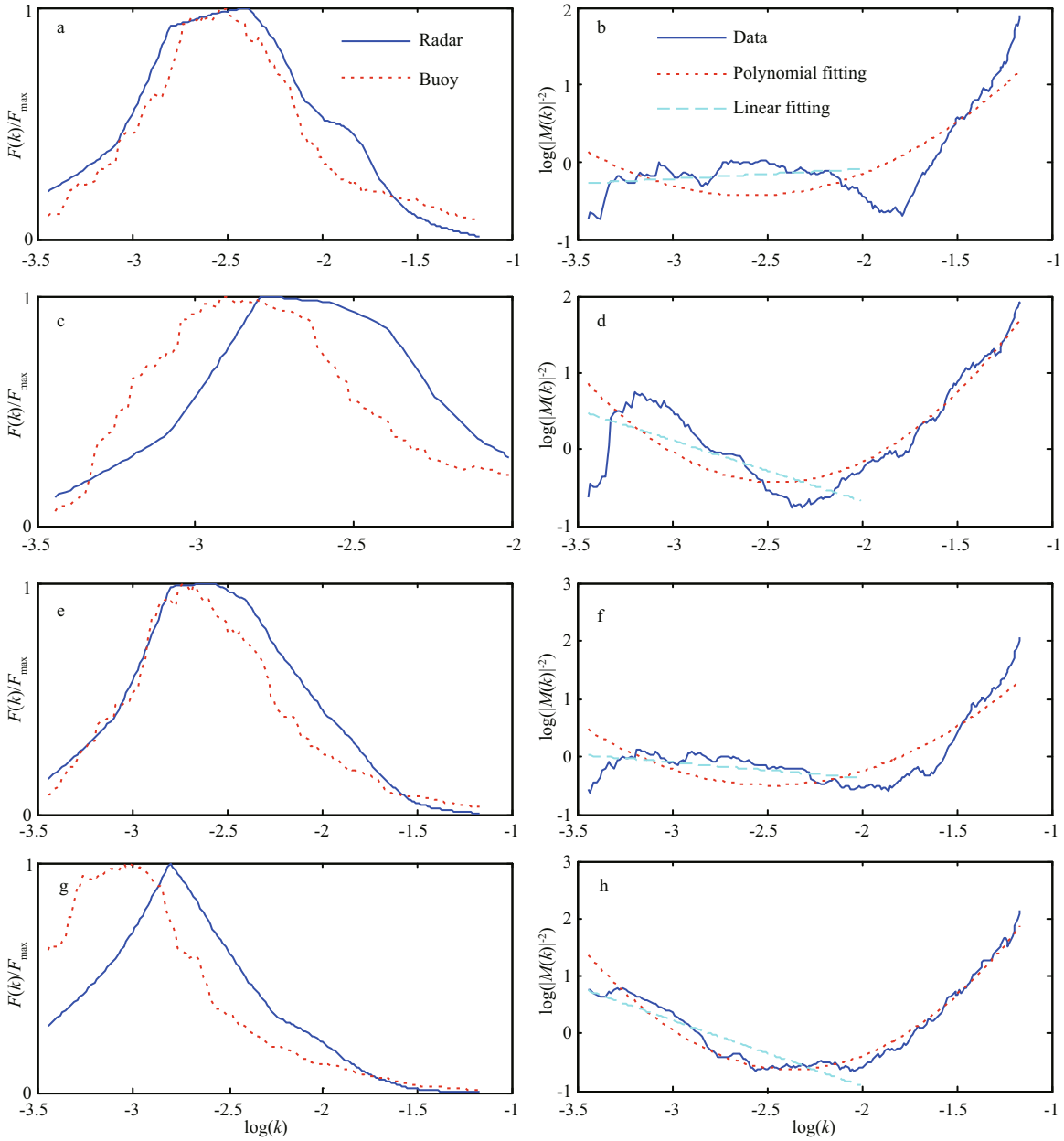

Fig.2 Left-hand panels: normalized 1D wavenumber frequency spectra derived from X-band marine radar image sequences (blue solid lines) and in situ buoy data (red dotted lines); right-hand panels: MTF estimated from experimental data (blue solid lines), fitted using a polynomial function (red dotted lines), and linear function (cyan dashed lines)

These are measured under four typical sea state conditions with different significant wave heights: a and b: 0.40 m; c and d: 1.51 m; e and f: 2.25 m; and g and h: 3.38 m.

where the exponent β must be determined by comparing the measurements from the radar and buoy.

When the MTF is derived, the 1D wave spectrum can be estimated using the following equation:

$$F_w(k) = F_r(k) \cdot |M(k)|^{-2}, \tag{10}$$

where subscript "w" denotes "wave" and $F_w(k)$ is the 1D wavenumber spectrum retrieved from the X-band marine radar image sequence. Ocean wave parameters such as peak wave period and mean wave period can be calculated using the 1D wave spectrum.

According to Eq.10, the 1D wave frequency spectrum can be obtained as follows:

$$F_w(\omega) = F_w(k)\frac{\mathrm{d}k}{\mathrm{d}\omega}, \tag{11}$$

where the peak wave period follows the well-known relation:

$$T_p = \frac{2\pi}{\omega_p}, \tag{12}$$

and ω_p is the peak angular frequency of $F_w(\omega)$. Therefore, the mean wave period can be simply derived as follows:

$$\overline{T}=\frac{2\pi\cdot\int_{\omega_1}^{\omega_2}F_w(\omega)\mathrm{d}\omega}{\int_{\omega_1}^{\omega_2}F_w(\omega)\omega\mathrm{d}\omega}, \quad (13)$$

where ω_1 and ω_2 are the lower and upper limits of the angular frequency range, determined by the temporal resolution of the radar image sequence and the temporal scale of the associated ocean waves.

3 EXPERIMENT AND VALIDATION

In this section, the experimental datasets are described and the proposed MTF validated using these data.

3.1 Experiment

An experiment was undertaken on Haitan Island, China. A description of the study area and the location of the X-band marine radar were introduced in an earlier study by Chen et al. (2014). The first period of the experiment (E_1) ran from December 22, 2012 to January 6, 2013, and the second (E_2) from January 12–18, 2013. E_1 ran for 364 hours, while E_2 ran for 156 hours. Figure 1 is a radar grayscale image captured during E_1. The wave direction and wavelength can be seen to vary as the wave propagates from east to west, such that the wave field in the observation area is heterogeneous.

A pitch-roll buoy was placed at a distance of 950 m from the radar station at an azimuth of 140° (shown by the green star in Fig.1). Every hour, the buoy recorded data from the 40th to the 57th minute at a sampling rate of 20 Hz. Three or four radar image sequences were recorded during this sampling period and to compare these with the radar retrievals and buoy measurements, the wave parameters retrieved from the radar image sequences were averaged.

A third experiment (E_3) was performed from October 31, 2013 to November 18, 2013. Two X-band marine radar systems (hereafter, named Radar 1 and Radar 2) were used to observe the same region simultaneously. The surroundings of experimental site and the configurations of Radar 1 were the same as in E_1 and E_2. The configuration of Radar 2 was the same as Radar 1, except the separation of the two radar antennas was 5 m in the horizontal direction and 3 m in the vertical direction. The two radar systems observed the same area of the ocean surface every 6 to 10 minutes to acquire one image sequence. In all, 1 432 radar image sequences were obtained by both radars during E_3. Unfortunately, there were no in situ buoy observations during E_3 and thus, the measurements of the two radar systems are used to evaluate the applicability of the proposed MTFs.

To validate the proposed MTFs, two different study regions were selected, as shown in Fig.1. Relative to the radar, Region 1 is 780–1 740 m and 125–150° in range and azimuth and Region 2, 667.5–1 627.5 m and 230–255°. The average water depths in Region 1 and Region 2 are about 28 and 15 m, respectively. Part of the radar image sequences of Region 1 were used to determine the unknown coefficients of the MTFs, and validate the retrieved ocean wave parameters utilizing the other parts of the radar image sequences in this region. Specifically, one radar image sequence of Region 1 was chosen at randomly from each hour of E_1 to determine the unknown coefficients of Eqs.8 and 9. Then, the remaining radar image sequences of E_1 and E_2 were used to retrieve the peak and mean wave periods. Finally, these values were compared with the measurements from the in situ buoy. However, as there were no buoy observations in Region 2, the radar image sequences acquired from the two radars in Region 2 are used to assess the applicability of the MTFs.

3.2 Result

Based on the radar image sequences from E_1, the coefficients of Eqs.8 and 9 are determined for each image sequence. Figure 3 illustrates the distributions of β, p_1, p_2, and p_3. Figure 3a shows that the exponent β in Eq.9 is normally distributed within the range of -2.6 to 1.8. Figure 3b–d shows that coefficients p_1, p_2, and p_3 of Eq.8 have distributions that are more tightly focused than that of β in Fig.3a, showing that the coefficients of Eq.8 might vary less with sea state than the coefficient in Eq.9. Therefore, to retrieve wave parameters by means of marine radar image sequences acquired with VV-polarization in nearshore regions, a quadratic polynomial MTF might be more suitable than the conventional linear MTF.

We then determine the average of each coefficient in Eqs.8 and 9 and obtain their respective mean values:

p_1=1.16, p_2=5.60, p_3=1.23,

and

β=-0.55

The peak and mean wave periods are easily estimated by utilizing two different MTFs (Eqs.8 and

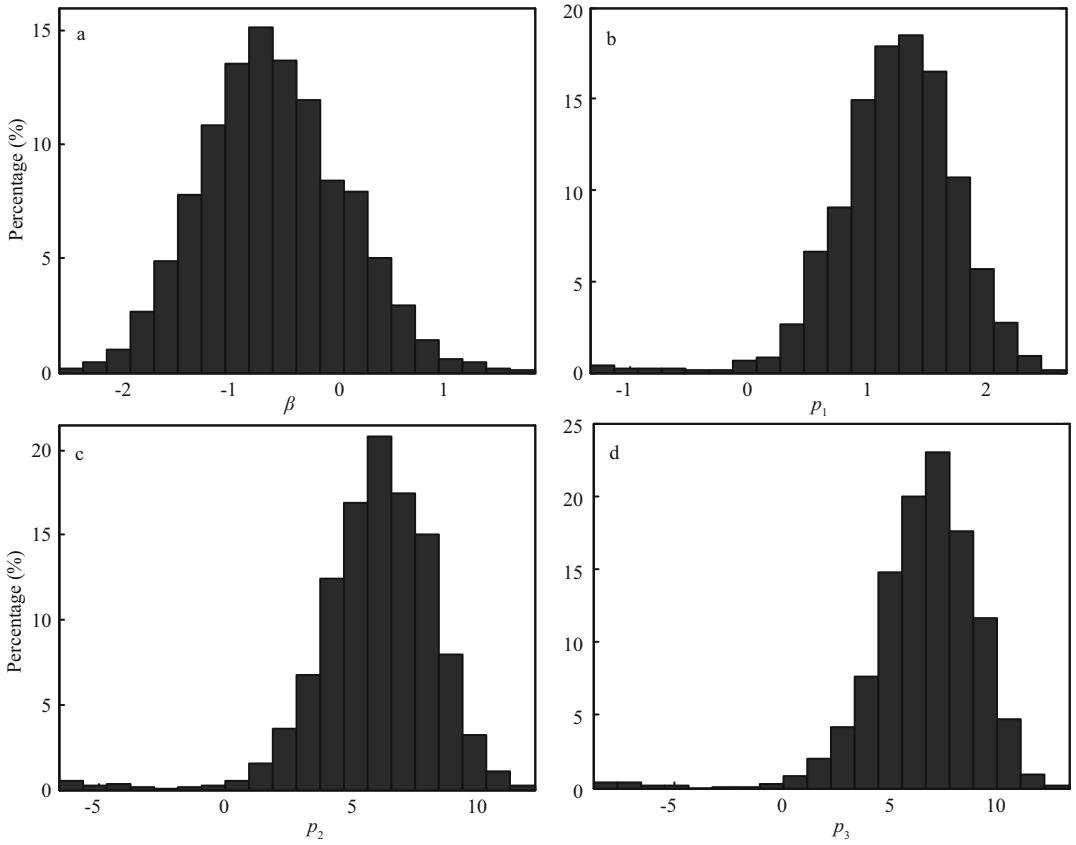

Fig.3 Histograms of the coefficients of the two MTFs

a. β; b. p_1; c. p_2; d. p_3.

9) and the radar image sequence. The retrieved values are compared with those measured by in situ buoy measurements. Figure 4a and c shows that the bias of the peak wave periods retrieved from the polynomial MTF is much smaller than from the linear MTF, whereas the root mean square error (RMSE) of the peak wave periods inversed from the former, is larger than from the latter. Figure 4b and d shows that both the bias and the RMSE of the mean wave periods from the quadratic polynomial MTF are smaller than from the linear MTF. Moreover, Fig.4d suggests that the bias of the mean wave period estimates occurs mainly when the period is less than 5 s, which might be caused by lower sea states and radar thermal noise.

We also compare the quadratic polynomial MTF proposed in this study with that of the conventional linear MTF derived by Nieto-Borge et al. (2004) (i.e., Eq.9 with β=-1.2), the results of which are summarized in Table 2. The retrieval accuracy of the peak and mean wave periods from the presented MTF are both better than the conventional linear MTF. The reason for this is that the former is derived from VV-polarization radar observations in shallow-water areas, while the latter is from HH-polarization radar observations in deep-water regions. The conventional linear MTF cannot be used directly to extract ocean wave parameters using X-band marine radar image sequences acquired in coastal waters. Table 2 also shows that the smallest bias and RMSE values of the mean wave periods might be achieved when the quadratic polynomial MTF is used. Thus, we suggest that the proposed quadratic polynomial MTF is suitable for the retrieval of the parameters of nearshore ocean waves from X-band marine radar image sequences.

Table 2 RMSE and bias between estimates of the peak and mean wave periods measured by the buoy and those retrieved from X-band marine radar image sequences using different MTFs

	RMSE of peak wave period (s)	RMSE of mean wave period (s)	Bias of peak wave period (s)	Bias of mean wave period (s)
β=-1.2	0.98	1.48	0.61	1.39
β=-0.55	0.74	1.03	0.24	0.93
Quadratic MTF	0.88	0.53	0.05	0.32

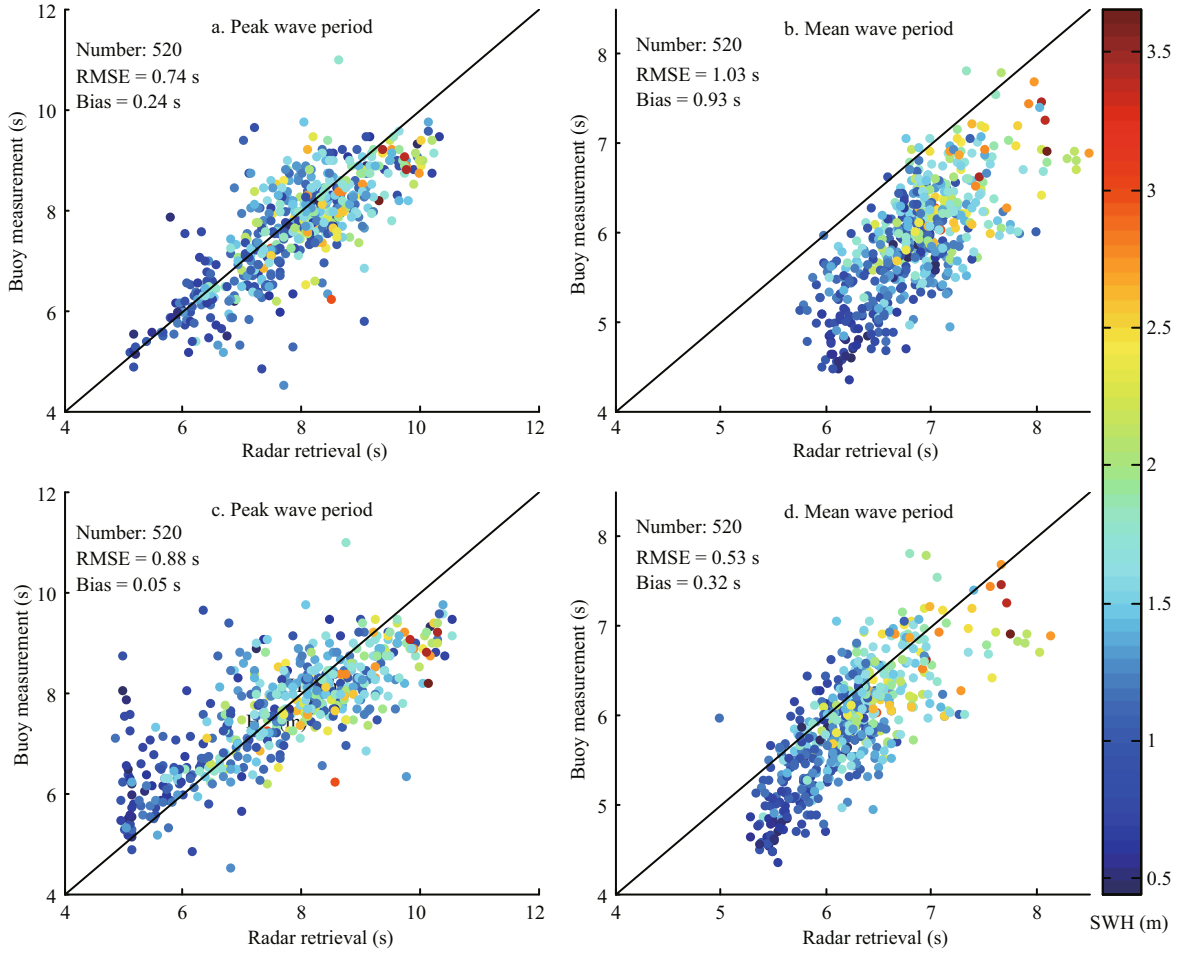

Fig.4 Comparison of the peak and the mean wave periods measured by the buoy and those retrieved from the X-band marine radar image sequences using different MTFs

a. peak wave period; b. mean wave period, as retrieved using linear MTF with β=-0.55; c. peak wave period; d. mean wave period, as retrieved using quadratic polynomial MTF. The different colored dots denote the different significant wave heights (SWH) measured by the buoy.

Moreover, the peak and mean wave periods retrieved from X-band marine radar image sequences under different sea states are compared with those measured by the in situ buoy, as shown in Table 3. The significant wave heights from the buoy observation characterize the sea states, which are divided into three bins: 0–1, 1–2.5, and 2.5–3.7 m. Table 3 shows that the proposed linear and quadratic polynomial MTFs have better performance than the conventional MTF under different sea states. Compared with the buoy measurements, the RMSEs of the peak wave period retrieved by the linear MTF (β=-0.55) are smaller than those retrieved by the quadratic polynomial MTF, while the RMSEs of the mean wave period retrieved by the former, are bigger than those derived by the latter. We suggest that it is suitable to retrieve peak and mean wave periods using the linear MTF and quadratic polynomial MTF, respectively. For three different sea states, the range of peak wave period RMSEs derived from the linear MTF is between 0.7 and 0.85 s, and it is between 0.98 and 1.23 s for the mean wave period RMSEs retrieved using the quadratic MTF. It is shown that the peak and mean wave periods RMSEs vary slightly for different significant wave heights, which indicates the proposed linear and quadratic polynomial MTFs are applicable to different sea states.

4 DISCUSSION

In this section, we discuss the effects of different MTFs on wave spectra retrieval, and the stability and suitability of the presented MTF.

4.1 Effect of MTF on the wavenumber spectra

To study the effects of the different MTFs on 1D wavenumber spectra retrieval, we compare the 1D wavenumber spectra derived directly from the radar

Table 3 Comparison of the peak and mean wave periods measured by the buoy and those retrieved from X-band marine radar image sequences under different sea states

SWH		β=-1.2	β=-0.55	Quadratic MTF
0–1 m	RMSE peak	1.35	0.76	0.99
	RMSE mean	1.69	1.23	0.63
	Bias peak	0.84	0.21	-0.53
	Bias mean	1.60	1.14	0.47
1–2.5 m	RMSE peak	0.84	0.70	0.74
	RMSE mean	1.40	0.98	0.51
	Bias peak	0.51	0.25	0.12
	Bias mean	1.32	0.88	0.29
2.5–3.7 m	RMSE peak	1.02	0.85	1.00
	RMSE mean	1.44	0.98	0.57
	Bias peak	0.87	0.58	0.76
	Bias mean	1.35	0.88	0.40

RMSEs and biases of the peak and mean wave periods are denoted as RMSE peak, RMSE mean, bias peak, and bias mean, respectively.

Table 4 Coefficients of MTF determined using the two datasets E_1 and E_2

	Dataset E_2	Dataset E_1
p_1	1.37	1.16
p_2	6.50	5.60
p_3	7.15	6.23
β	-0.79	-0.55

image spectrum without any MTF, as well as those estimated using the two MTFs with the corresponding wave spectrum determined by the in situ buoy measurements. Figure 5 shows that the peak wavenumber derived from the radar image spectrum (blue solid line) is close to that of the buoy measurement (red dotted line). A difference between the 1D wavenumber from the marine radar imagery and the corresponding spectra from the buoy can be observed, which is caused by the radar wave imaging mechanism (shadowing and/or tilt modulation); however, this difference can be minimized by an MTF.

The retrieved 1D wavenumber spectrum using the linear MTF appears to agree relatively well with that measured by the buoy at the lower wavenumbers, whereas notable deviations exist where wavenumbers are greater than 0.08 rad/m. By comparison, the 1D wavenumber spectrum estimated using the quadratic polynomial MTF is similar to that of the linear MTF at the wavenumbers near the peak of the spectra (i.e.,

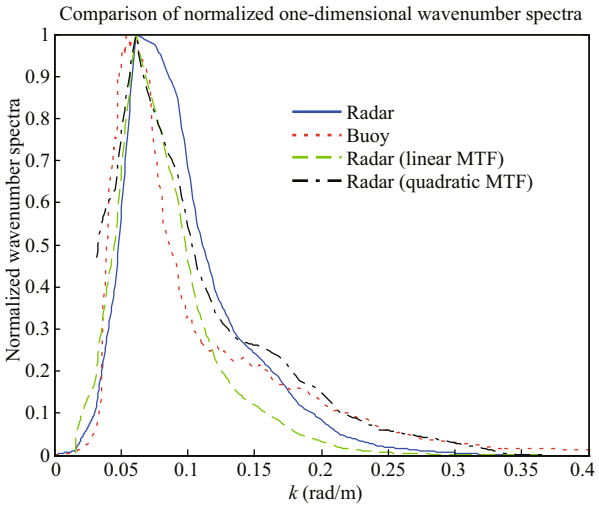

Fig.5 Comparison of normalized 1D wavenumber spectra from the in situ buoy measurements and those retrieved from the X-band marine radar image sequences using different MTFs

wavenumber range of 0.05–0.08 rad/m), and it corresponds very well with the buoy spectrum at high wavenumbers (i.e., wavenumber is approximately greater than 0.2 rad/m). However, in the rear face of the spectrum (i.e., wavenumber range of 0.08–0.2 rad/m), both wavenumber spectra retrieved using the two MTFs have notable deviations from the buoy spectrum.

The mean wave period is calculated from the integral of the entire 1D wavenumber spectrum between the low and high wavenumber regions. It is therefore suitable to use the quadratic polynomial to estimate the mean wave period, rather than the peak wave period. Table 2 shows that the mean wave period retrieved using the quadratic polynomial MTF provides the best results.

4.2 Stability of the proposed MTF

In Section 3.2, the coefficients of Eqs.8 and 9 are determined using parts of the X-band marine radar image sequences acquired in E_1. To validate the stability of the proposed MTF, we also use corresponding data from E_2 to derive the coefficients. One radar image sequence is selected from each hour of dataset E_2, and the coefficients of Eqs.8 and 9 obtained using the method presented in Section 2.2, as shown in Table 4.

After determining the MTF coefficients, the peak and mean spectral periods are retrieved from the remaining X-band marine radar image sequences. Table 5 summarizes the comparison between the peak

Table 5 RMSEs and biases between the peak and mean periods measured by the buoy and retrieved from X-band marine radar image sequences, resulting from E_2 for the determination of the coefficients of the MTF

	RMSE of peak wave period (s)	RMSE of mean wave period (s)	Bias of peak wave period (s)	Bias of mean wave period (s)
β=-0.79	0.82	1.20	0.38	1.10
Quadratic MTF	0.89	0.54	0.16	0.34

Table 6 RMSEs and biases of the peak and mean wave periods estimated using image sequences acquired from Radar 1 and Radar 2 during experiment E_3, and the conventional and proposed MTFs

	RMSE of peak wave period (s)	RMSE of mean wave period (s)	Bias of peak wave period (s)	Bias of mean wave period (s)
β=-1.2	0.30	0.09	-0.02	0
β=-0.55	0.28	0.09	0	0.03
Quadratic MTF	0.41	0.11	0.03	0.06

and mean periods estimated with the two MTFs, as well as those measured by the buoy. It can be seen that the RMSE and bias of the peak wave periods derived from the linear MTF (β=-0.55) are relatively close to those from the quadratic polynomial MTF. However, the RMSE and bias of the mean wave period estimated from the quadratic polynomial MTF are much smaller than those calculated with the linear MTF (β=-0.55). These results are consistent with those shown in Table 2. Tables 4 and 5 show that although the coefficients are different for the linear or quadratic polynomial MTFs, the RMSEs and biases of the peak and mean wave periods retrieved from the radar image sequences are similar. Therefore, it is shown that the proposed MTF is stable.

4.3 Applicability of the proposed MTFs

To evaluate the applicability of the proposed MTFs for different X-band marine radar systems, the radar image sequences acquired by Radar 1 and Radar 2 during E_3 are used to retrieve the peak and mean wave periods. Table 6 shows the RMSEs and biases of the peak and mean wave periods estimated using image sequences acquired from Radar 1 and Radar 2 during the experiment, and the conventional and proposed MTFs. It is shown that the RMSEs and biases of the peak or mean wave period derived from the different MTFs are similar. Therefore, we suggest that the proposed MTFs are insensitive to different radar systems. Because of the lack of buoy observations in Region 1 and Region 2, we cannot assess whether the proposed MTFs are suitable for application in different areas or not.

5 CONCLUSION

X-band marine radar imaging of ocean surface waves is affected by nonlinear modulation processes. Therefore, there are differences between the image spectra derived from radar image sequences and in situ spectra measured by buoys. To retrieve the ocean wave parameters from radar observations, an MTF is used to minimize these differences. This paper proposes a new quadratic polynomial MTF for X-band marine radar acquisition of data at grazing incidence and VV polarization. The proposed MTF is used to retrieve the peak and mean wave periods. The RMSE and bias between peak wave periods measured by in situ buoys and those retrieved from radar image sequences using the quadratic polynomial MTF are 0.88 and 0.05 s, respectively, which are similar to those estimated with the linear MTF. However, the RMSE and bias of the mean wave periods retrieved using the quadratic polynomial MTF are 0.53 and 0.32 s, respectively, which are more accurate than calculated with the linear MTF.

There are evident differences between the new proposed quadratic polynomial MTF and the linear MTF presented by Nieto-Borge et al. (2004). The presented MTF is derived from VV-polarized radar observations in a relatively shallow nearshore region, whereas the linear MTF described by Nieto-Borge et al. (2004) is obtained from HH-polarized radar data from deep water in an offshore area. In the nearshore region, the ocean wave field is heterogeneous because of shoaling waves and wave reflections from the shore. Therefore, the linear MTF is not suitable for the extraction of ocean wave parameters using X-band marine radar image sequences acquired in coastal areas.

6 ACKNOWLEDGEMENT

We thank the two anonymous reviewers for their constructive comments, which helped us greatly in improving the manuscript.

References

Alpers W R, Ross D B, Rufenach C L. 1981. On the detectability of ocean surface waves by real and synthetic aperture

radar. *Journal of Geophysical Research*, **86**(C7): 6 481-6 498.

Chen Z B, He Y J, Zhang B, Qiu Z F, Yin B S. 2014. A new algorithm to retrieve wave parameters from marine X-band radar image sequences. *IEEE Transactions on Geoscience and Remote Sensing*, **52**(7): 4 083-4 091, http://dx.doi.org/10.1109/TGRS.2013.2279547.

Cui L M, He Y J, Shen H, Lü H B. 2010. Measurements of ocean wave and current field using dual polarized X-band radar. *Chinese Journal of Oceanology and Limnology*, **28**(5): 1 021-1 028, http://dx.doi.org/10.1007/s00343-010-9056-8.

Dankert H, Horstmann J. 2007. A marine radar wind sensor. *J. Atmos. Oceanic Technol*., **24**(9): 1 629-1 642.

Lee P H Y, Barter J D, Beach K L, Hindman C L, Lake B M, Rungaldier H, Shelton J C, Williams A B, Yee R, Yuen H C. 1995. X Band microwave backscattering from ocean waves. *J. Geophys. Res*., **100**(C2): 2 591-2 611.

Nieto-Borge J C, Hessner K, Jarabo-Amores P, de la Mata-Moya D. 2008. Signal-to-noise ratio analysis to estimate ocean wave heights from X-band marine radar image time series. *IET Radar*, *Sonar and Navigation*, **2**(1): 35-41.

Nieto-Borge J C, Rodríguez G R, Hessner K, González P I. 2004. Inversion of marine radar images for surface wave analysis. *Journal of Atmospheric and Oceanic Technology*, **21**(8): 1 291-1 300.

Nieto-Borge J C. 1997. Analisis de Campos de Oleaje Mediante Radar de Navegacion en Banda X. Ph.D. thesis. University of Madrid, Madrid, Spain. 320p.

Plant W J. 1988. The modulation transfer function: Concept and applications. *In*: Komen G J, Oost W A eds. Radar Scattering from Modulated Wind Waves. Springer, Netherlands. p.155-172.

Seemann J. 1997. Interpretation der Struktur des Wellenzahl-Frequenzspektrums von Radar-Bildsequenzen. Ph.D. thesis. Universität Hamburg. 257p.

Senet C M, Seemann J, Flampouris S, Ziemer F. 2008. Determination of bathymetric and current maps by the method DiSC based on the analysis of nautical X-band radar image sequences of the sea surface. *IEEE Transactions on Geoscience and Remote Sensing*, **46**(8): 2 267-2 279.

Trizna D B. 1997. A model for Brewster angle damping and multipath effects on the microwave radar sea echo at low grazing angles. *IEEE Transactions on Geoscience and Remote Sensing*, **35**(5): 1 232-1 244.

Wenzel L B. 1990. Electromagnetic scattering from the sea at low grazing angles. *In*: Geernaert G L, Plant W J eds. Surface Waves and Fluxes. Springer, Netherlands. p.109-171.

Young I R, Rosenthal W, Ziemer F. 1985. A three-Dimensional analysis of marine radar images for the determination of ocean wave directionality and surface currents. *J. Geophys. Res*., **90**(C1): 1 049-1 059.

Ziemer F, Gunther H. 1994. A system to monitor ocean wave fields. *In*: Proc. Second Int. Conf. on Air-Sea Interaction and Meteorology and Oceanography of the Coastal Zone. Amer. Metetor. Soc., Lisbon, Portugal. p.18-19.